eNeuro

Research Article: New Research
Sensory and Motor Systems

Acute Loss of Tactile Input Leads to General Compensatory Changes in Eye–Hand Coordination during Object Manipulation

Kevin Ung,[1] John F. Magnotti,[2] Brandon Kim,[1] Jeffrey M. Yau,[1] and Per F. Nordmark[3]

[1]Department of Neuroscience, Baylor College of Medicine, Houston, Texas 77030, [2]Department of Neurosurgery, Perelman School of Medicine, University of Pennsylvania, Philadelphia, Pennsylvania 19104, and [3]Department of Medical and Translational Biology, and Department of Diagnostics and Intervention, Section for Hand and Plastic Surgery, Umeå University, Umeå 901 87, Sweden

Abstract

Current models of motor control emphasize the critical role of sensory feedback, as demonstrated by movement coordination deficits following sensory impairment. When both vision and touch are available for object-oriented manual behaviors, they serve distinct roles; vision guides the execution of planned movements, while touch provides more direct feedback on hand–object interactions. The impact of losing somatosensory feedback on eye–hand coordination during dexterous object manipulation tasks has not been thoroughly studied. Conceivably, vision is recruited to compensate for the feedback lost when touch is abolished based on the dexterity demands of the behavior. To investigate this, we tested healthy participants of either sex on a manual dexterity task requiring the movement of small metal pegs, both before and after the administration of digital anesthesia, which selectively abolished cutaneous sensations in the fingertips while preserving motor function. We recorded participants' gaze and hand positions. Despite loss of cutaneous feedback, participants successfully completed the pegboard task. However, they exhibited significantly longer trial times and altered force profiles. Notably, acute somatosensory loss triggered a rapid shift in visual behavior, characterized by a tighter coupling between gaze and hand positions across all task actions, even those not directly involving object manipulation. These changes, which occurred with anesthesia of the dominant and nondominant hands, were not evident with sham (saline) injections. Our findings underscore the contributions of sensory feedback to force control in service of dexterous object manipulation and reveal the nonselective nature of compensatory gaze–hand coordination processes.

Key words: digital anesthesia; eye-hand coordination; manual dexterity; sensorimotor integration; somatosensory feedback; visual compensation

Significance Statement

Touch and vision typically support distinct but coordinated aspects of dexterous manual behaviors. Here, we evaluated how acute removal of tactile feedback using digital anesthesia affected performance and gaze–hand coordination in a manual dexterity task. With insensate fingers and intact vision, participants continued to perform the task successfully, albeit with marked longer trial times and altered force profiles. We also observed closer alignment between gaze and hand positions during all task actions, even those that did not involve object manipulation. Our results reveal the consequences of acute somatosensory loss and the general nature of compensatory eye–hand coordination processes.

Received Nov. 21, 2023; revised Aug. 22, 2025; accepted Aug. 30, 2025.

The authors declare no competing financial interests.

Author contributions: P.F.N. designed research; K.U., J.F.M., B.K., J.M.Y., and P.F.N. analyzed data; K.U., J.F.M., J.M.Y., and P.F.N. wrote the paper.

We express our gratitude to Göran Westling, Anders Bäckström, and Kamil Antos for their invaluable contributions to hardware and software development and technical support. We extend our appreciation to Carola Hjälten for her dedicated efforts in data collection, and we are especially thankful to Roland S. Johansson for his profound insights and assistance in refining the assessment paradigm. We also thank all volunteers for their participation in the study. This work was financially supported by the Västerbotten County Council, Sweden and the NeuralCODR Postdoctoral Training Fellowship awarded to K.U. (T32NS125115).

Continued on next page.

Introduction

Dexterous manual interactions with objects require coordination between sensory and motor systems. When all sensory channels are available, vision and touch support

complementary roles: vision provides information that supports grasping and movement planning (Johansson et al., 2001), while touch provides direct feedback for performance monitoring and error correction (Johansson and Flanagan, 2009). When tactile sensory inputs are diminished or lost, the available input channels from vision may be recommissioned to fill in critical information gaps.

Touch is crucial for perceiving hand posture, movements, and the physical interactions between the hand and grasped objects (Johansson and Flanagan, 2009). Tactile signals from proprioceptors and cutaneous mechanoreceptors inform grasped objects' properties, including shape (Johnson and Hsiao, 1992; Jenmalm et al., 2003), grip force adaptation (Jenmalm et al., 2000), alignment of fingertips (Monzée et al., 2003), and texture or friction (Johansson and Westling, 1984; Sathian et al., 1989; Bilaloglu et al., 2016). Additionally, touch provides real-time feedback about forces (Johansson and Westling, 1987), friction, and slip events during object manipulation (Johansson and Westling, 1987; Birznieks et al., 1998). The absence or reduction of tactile feedback disrupts these critical functions, leading to impaired manual dexterity and object manipulation deficits.

Vision, while less directly involved in signaling mechanical interactions, supports manual tasks by providing information critical for object localization (Johansson et al., 2001), shape inference, and contextual cues for prehension (Gordon et al., 1993; Jenmalm and Johansson, 1997; Jenmalm et al., 2000; Winges et al., 2003; Lukos et al., 2007; Johansson and Flanagan, 2009). Gaze direction is integral to planning and monitoring visually guided actions (Johansson et al., 2001; Sailer et al., 2005). Individuals who have suffered nerve injuries affecting fingertip sensation often express a greater reliance on visual feedback when engaging in dexterous object manipulation tasks (Blouin et al., 1996; Vercher et al., 1996; Stenneken et al., 2006). Nerve injury is also associated with increased gray matter volume in regions of visual association cortex linked to eye–hand coordination, consistent with an increased dependence on vision to compensate for reduced somatosensory input (Nordmark et al., 2018). Such compensatory changes may be considered a form of sensorimotor learning, where the brain adapts to sensory deficits by modifying feedback processing.

Effective sensorimotor behavior requires the association of actions and their sensory consequences. Severe deafferentation such as for an entire limb or the whole body is known to cause changes in gross motor function, timing of movements, and prehension (Gentilucci et al., 1994, 1997; Blouin et al., 1996; Cuadra et al., 2019). Individuals who have lost their somatosensory and proprioceptive feedback develop movement disorders (Rao and Gordon, 2001; Chesler et al., 2016; Mahmud et al., 2017; Yahya et al., 2019) and ultimately compensate for the loss of input through other mechanisms (Jenmalm and Johansson, 1997; Augurelle et al., 2003; Monzée et al., 2003; Trillos et al., 2018). However, basic motor tasks such as lifting an object, holding it, and lowering it to the surface may still be performed well as sufficient force to maintain grasping the object can be produced simply by applying more force (Jenmalm et al., 2000). Motor movements can sometimes be informed by the context in which the movement occurred, based on the goal and the sensory information available (Sober and Sabes, 2005). With hand–object interactions, visual processing that typically subserves reaching and grasping may be recruited to provide feedback to compensate for missing or impoverished somatosensory signaling. Whether this compensation is restricted to specific task states (i.e., evaluating whether an object is successfully grasped) or generalizes across contexts is unknown.

In two experiments, we asked how the loss of tactile feedback in the fingers affects gaze behavior during a fine motor task testing manual dexterity and whether compensatory gaze changes are specific or generalized. To address these questions, we tracked hand movements and gaze direction as participants performed a pegboard test that required the collection, transport, and placement of small pegs. We assessed performance before and after we abolished tactile feedback through local anesthesia of the digits. We hypothesized that the loss of somatosensory feedback would induce compensatory gaze changes that were specific to only action contexts involving precise object manipulation. We found that removal of tactile feedback perturbed performance which visual compensation only partially rescued. Notably, compensatory gaze changes were not restricted to specific actions in the pegboard task and instead reflected a general yoking of gaze to the anesthetized hand. These behavioral changes, which were minimal with saline injections, occurred with anesthesia of the nondominant hand (Experiment 1) and dominant hand (Experiment 2).

Correspondence should be addressed to Jeffrey M. Yau at jeffrey.yau@bcm.edu or Per F. Nordmark at per.nordmark@umu.se.

Materials and Methods

Participants. Eleven healthy individuals participated in the study (mean age, 29 years; range, 23–42 years; four females). Ten participants were right-hand dominant (Edinburgh inventory, laterality index 70–100; Caplan and Mendoza, 2011) and one left-hand dominant (−80). Eight of the participants were right-eye dominant, two left-eye dominant, and one bilaterally dominant. All participants had normal or corrected-to-normal vision.

Five participants performed the task (Experiment 1) under baseline (no sham or anesthesia) conditions and after digital anesthesia to the nondominant hand. A separate sample of six participants performed the identical task (Experiment 2) under baseline conditions, saline injection to the dominant hand (sham), and digital anesthesia to the dominant hand. Beyond serving as a replication study, Experiment 2 provided the opportunity to control for potential hand dominance. Data related to gaze position for one participant in Experiment 2 were dropped from analyses due to a technical problem with gaze tracking.

All participants gave their written informed consent in accordance with the Declaration of Helsinki, and the Swedish Ethics Review Authority approved the study (Dnr 2021-06981-01). No participants reported a history of nerve disorders or diabetes. All participants were paid for their participation (500 SEK).

General overview. The participants performed a dexterous unimanual task comprising the collection, transport, and delivery of pegs (Fig. 1*A*). A fixed forehead support defined the individual location of the head and eyes during performance of the task. Gaze and hand positions in the workspace were recorded throughout the performance of the task using recording devices mounted in fixed positions on a height-adjustable desk (Fig. 1*B*). A monitor (480 × 270 mm) defined the depth of the workspace and displayed written instructions to the participant during the tasks. A 90 mm deep shelf with collection (outer) trays and the pegboard (middle) tray was mounted 165 mm from the top of the computer screen, serving as the basis for the workspace. Force transducers registered normal and torque forces produced by the participants' unimanual actions on each of the trays. The defined workspace for the acting hand during the task was limited to an area ∼40 cm in front and 10 cm below the eyes (for the left hand, from centered to ∼20 cm left of a midpoint between the eyes, and respectively to the right for the right hand). Table height was adjusted to each participant enabling them to stand while performing the task. The workspace areas were defined to maximize comfort for the participant while minimizing occlusion of gaze position tracking. Black fabric covered the tabletop and screens mounted on its back and sides to prevent potential distortion of gaze and hand position tracking by reflective light. For the same reason, the participants wore sleeves of black fabric covering their arms down to the wrist level.

Pegs and peg holes. Each peg consisted of a smooth metal rod (duralumin, diameter, 6 mm; length, 32 mm; weight, 7.6 g). All pegs had uniform color, shape, and weight. Peg holes (diameter, 6.5 mm; depth, 10 mm) were arranged in two rows on a plastic 3D-printed surface (85 × 75 mm). Each row was separated by 23 mm, and peg holes within a row were separated by 13 mm. The front row was 65 mm from the computer monitor.

Collection trays. The collection trays, one on the left and one on the right side of the peg holes, were 3D-printed plastic concave discs with a 6 cm diameter. The ridge of the disc was aligned with that of the ledge, and the central part of the disc featured a flat surface with a 2 cm radius, situated 7 mm below the outer edge. We designed the tray in this way so that the participants were required to grasp the peg using a precision grip. Before the start of each series of trials, eight pegs were placed flat in the collection tray such that no peg was on top of another peg.

Gaze position tracking. A gaze tracker (The EyeTribe tracker; sampling rate, 30 Hz) was mounted centered below the workspace facing the eyes of the participant (Fig. 1*B*). For each participant, before the start of the data registration for each round, the gaze tracker was calibrated using the device's standard nine-point calibration procedure. For data analysis, we used the average coordinate registered for the two eyes.

Hand position tracking. The device for tracking hand motion (Leap Motion Controller; sampling rate, 120 Hz) was mounted centered 40 cm above the workspace (Fig. 1*B*). The setup was optimized to ensure that the entire workspace for peg placement and retrieve movements remained well within the calibrated tracking volume. Before the start of data registration, the device's ability to identify the hand, thumb, and index and middle finger coordinates were confirmed by the experimenter. Participants removed all jewelry and watches prior to the experiment to facilitate tracking. The hand tracking data were aligned with the eye tracking data to a common two-dimensional reference frame in the plane of the computer screen using a custom-made script. This established a unified coordinate system for the sampled hand and gaze coordinates in the plane of the computer screen, positioned 3.5–6.5 cm beyond the first and second row of peg holes from the perspective of the subjects' eyes.

Force transducers. Force transducers (load cell weight sensors, TZT HX711 Module Electronic Scale Aluminum Alloy Weighting Pressure Sensor, 1 kg, 1,600 Hz) registered normal and torque forces applied to the pegboard tray and two collection trays. Continuous sampling from all devices enabled the registration of task-related force variations to eye and hand positions throughout the task (Fig. 1*C*).

Additional sensors. Light sensors (sampling rate, 1,600 Hz) were mounted in concave 3D-printed plastic handrests (half spheres; radius, 3 cm). Participants placed their left and right hands in separate handrests at the start of each series. The light sensors were used to confirm the movement onset and offset times for the active hand on each series. The light sensors also served to confirm the stationary status of the passive hand throughout the series.

Procedure. Each experiment (Fig. 1*D*) comprised multiple blocks defined according to the state of the hand receiving the injections (Experiment 1, nondominant hand; Experiment 2, dominant hand). Experiment 1 comprised two blocks: baseline (no intervention) and anesthesia. Experiment 2 comprised three blocks: baseline, sham injection, and anesthesia. Injections (see below) were performed immediately following Block 1 in Experiment 1 and Blocks 1 and 2 in Experiment 2. Basic sensory and motor capabilities (see below) were evaluated prior to each block and following the final block.

Each block consisted of testing of the dominant and nondominant hands. Each hand was tested in four rounds consecutively. Participants were offered a short break (1–3 min) between rounds. Gaze and hand position tracking calibration was performed prior to the start of each round. Data were continuously recorded over each round.

Each round comprised five series. At the start of each series, the hands were placed on top of handrests equipped with light sensors. Series were divided into placement and retrieval phases. An acoustic signal indicated when participants should begin each phase. During the placement phase, participants moved the pegs, one at a time, from the tray to the peg holes. The collection and delivery of a single peg defined a placement trial. After placing all eight pegs, participants returned the active hand to the handrest. After a 4 s pause, an acoustic signal prompted participants to begin the retrieval phase. During the retrieval phase, participants moved the pegs, one at a time, from the peg holes to the collection tray. The collection and return of a single peg defined a retrieval trial. After returning all the pegs to the collection tray, participants placed the active hand back on the handrest to signal the end of the series.

Participants were instructed to use a precision grip to grasp and place the pegs. No instructions were given regarding how to collect the pegs (other than one at a time), regarding the order of the pegs, or regarding gaze direction (i.e., the participants were free to find their own strategy). If a peg was dropped, participants were instructed to continue by picking up a new peg and leaving the dropped peg for last.

In Experiment 1, each participant performed 1,280 total trials. In Experiment 2, each participant performed 1,920 total trials.

Digital anesthesia and saline control injections. In both experiments, digital anesthesia was performed by a hand surgeon (author P.F.N.) experienced in regional anesthesia in the hand and arm. We regionally anesthetized the three digits of the hand involved in dexterous manipulation: the thumb, the index finger, and the middle finger. To induce an immediate and persistent digital anesthesia effect, we used a 1:1 mix of the fast-onset local anesthetic lidocaine (1%) and the long duration local anesthetic levobupivacaine (0.5%). A 1.5 ml volume of this local anesthetic mix was injected in each of the addressed fingers with a volar approach through a 27 gauge needle, with the participants in supine posture. For the six participants tested in Experiment 2, isotonic saline injections (1.5 ml volume of 0.9% NaCl isotonic saline) were performed to their dominant hand in the manner described for the digital anesthesia immediately following the completion of the baseline testing blocks.

Evaluating basic motor and sensory capabilities. Motor and sensory functions of the fingers on the manipulated hand were evaluated at the start of the test sessions (prior to the baseline blocks), prior to the testing blocks that followed the sham and anesthesia injections, and at the end of test sessions (after the anesthesia blocks). Accordingly, the fingers on the nondominant hand were evaluated three times in Experiment 1, and the fingers on the dominant hand were evaluated four times in Experiment 2. These qualitative evaluations were intended as gross characterizations of participants' sensory and motor functions before and after the interventions. We found that participants' range of motion (ROM) for the thumb, index finger, and middle finger were unchanged by the sham and anesthesia injections compared with baseline ROM. In contrast, anesthesia resulted in an extreme loss of sensation for sharp touch in all participants as characterized the static two-point discrimination (2PD) test (measured in the radial and ulnar half of volar fingertip for thumb, index finger, and middle finger). Specifically, all participants had typical 2PD thresholds ranging from 3 to 4 mm prior to the baseline blocks (in Experiments 1 and 2) and after sham injection (in Experiment 2). After anesthesia, we were unable to measure 2PD thresholds which exceeded the maximum testing range of our measurement device (15 mm) in all participants. Thresholds continued to exceed 15 mm when assessed at the end of the anesthesia blocks. There were no adverse effects, and all participants were able to complete the task after digital anesthesia.

Data curation. From the continuously recorded data, we segmented the placement and retrieval phases into discrete collection, transport, and delivery actions objectively using the normal force signals measured at the pegboard and collection trays. Collection action onset was defined as a change point as detected by the Primed Exact Linear Time (PELT) method (Killick et al., 2012) in the normal force (measured at the collection tray or pegboard), and collection action offset was defined by a change point with a return of normal force to baseline levels. Delivery action onset was defined as a change point in the normal force (measured at the pegboard or collection trays) detected by the PELT method, and delivery action offset was defined by a change point with a return of normal force to baseline levels. Change points were then manually inspected and corrected as needed. Transport actions were defined by each collection offset time and the subsequent delivery onset time. Because the weight of the delivered pegs introduced a consistent and accumulating offset to the force transducer

measurements over the series, we computed the offset pattern and detrended this pattern from the entire series such that the forces associated with the start of trial were re-centered to 0. The baseline was defined as the average of the onset and offset points after detrending. In Experiment 1, our system failed to record torque force data on a subset of trials. These failures were only identified after data collection, and these trials were excluded from the torque force analysis.

Data analysis. Analyses were performed using MATLAB (R2023a) and RStudio (R version 2024.12.0 + 467) on a MacBook Pro running macOS Sonoma 14.6.1. We first characterized the impact of digital anesthesia on the performance speed and forces produced during peg collection, transport, and delivery in order to relate our work to prior studies (Gentilucci et al., 1997; Jenmalm et al., 2000; Augurelle et al., 2003). Our analyses distinguished between trials involving peg collection from the large collection trays with delivery to the small peg holes (precise delivery) and trials with collection from peg holes with delivery to the large collection trays (coarse delivery). This distinction allowed us to test the hypothesis that gaze–hand position relationships depend on the action being performed. To determine the impact of digital anesthesia, we quantified action durations (difference between onset and offset times), peak normal force, and total torque force. We also quantified peg transport durations (time elapsed from collection offset to delivery onset) and hand movement durations without pegs (time elapsed from delivery offset to collection onset). We report times rounded to the nearest hundredth of a millisecond and force to the nearest thousandth of a Newton or Newton meter for normal and torque force, respectively. We defined the forces from the acting hand in downward direction against the tray/peg holes as positive normal forces and computed absolute values to quantify normal force magnitude. To quantify torque force, we similarly computed the absolute value to estimate total force irrespective of direction along the recorded axis.

To determine how digital anesthesia modulated gaze–hand position relationships, we quantified the spatial separation between gaze position and index finger position during peg collection, transport, delivery actions, and during peg-free hand movement. Given the configuration of the pegboard and collection trays, most of the positional variance during task performance was confined to the horizontal axis, so we computed the distance between the gaze position and index finger position (gaze-index separation index, GISI) in the *x*-axis. In separate analyses, we confirmed that positional variance in the *y*-axis was limited and variance in distance metrics computed in two dimensions was dominated by the variance in the horizontal dimension. For collection and delivery actions, GISI was calculated during the time of peak normal force and as a function of normalized progress through the actions defined as the percentage of the full action duration (action progress, AP). To normalize the percentage progress through actions, we split the progress into quartiles using a snapshot of the point coinciding with the quartile based on the range between action onset (0% progress) and offset (100% progress) as demarcated by force plate readings. GISI was similarly calculated as a function of normalized progress over the peg transport and peg-free hand movement actions. Separate analyses were performed for actions extracted from the placement and retrieval trials. To quantify the changes in GISI within a hand, we calculate the difference of GISI between baseline and treatment (ΔGISI). To evaluate how ΔGISI differed between the dominant and nondominant hand, we computed the difference of the ΔGISI metric between hands (ΔΔGISI). This analysis approach enables us to quantify the effect of our interventions while accounting for potential learning or fatigue effects related to the passage of time.

We statistically assessed how force, duration, and GISI were modulated according to hand and condition block (baseline, sham, anesthesia blocks) using linear mixed-effect models from the *lme4* package (Bates et al., 2015). To test modulation of force, duration, and GISI at peak force, we included block (Experiment 1, baseline vs postanesthesia; Experiment 2, baseline vs sham vs anesthesia) and hand (dominant vs nondominant) as fixed effects. To account for subject-specific variance and learning effects, we included series nested within subject as a random effect on the slope. Thus, the model for any dependent variable (DV) took the following form:

$$\mathrm{DV} = \mathrm{Block} * \mathrm{Hand} + (1|\mathrm{Subject}/\mathrm{Round}).$$

We similarly tested modulation of GISI as a function of normalized progress by including percentage progress through the action as an additional fixed effect. The model took the following base form:

$$\mathrm{GISI} = \mathrm{Block} * \mathrm{Hand} * \mathrm{Progress} + (1 + \mathrm{Block} * \mathrm{Hand} * \mathrm{Progress}|\mathrm{Subject}) + (0 + \mathrm{Round}|\mathrm{Subject}).$$

We used the *car* package (Fox et al., 2001) to estimate the statistical significance for all fixed effects (Type 2 Wald χ^2 tests). Post hoc tests were calculated using the *emmeans* package (Searle et al., 1980; Lenth, 2017), which applies multiple-comparison correction (Tukey's test). Because of the large number of trials across participants, we followed the package recommendation to use the asymptotic method for degrees of freedom for the post hoc tests.

To statistically assess for an effect of learning, we again modeled the hand and block as fixed effects along with the series within a block ($\mathrm{Series}_{\mathrm{Block}}$). $\mathrm{Series}_{\mathrm{Block}}$ accounted for previous experience within a block, thus examining learning through a given condition. We applied this model to force duration and GISI at peak force as DVs to determine the slope as a measure of learning:

$$\mathrm{DV} = \mathrm{Block} * \mathrm{Hand} * \mathrm{Series}_{\mathrm{Block}} + (1|\mathrm{Subject}/\mathrm{Round}).$$

The trend (slope) of the DV was calculated with the emtrends function from the emmeans package to evaluate how the response changes with respect to $\text{Series}_{\text{Block}}$.

For a complementary analysis of the spatiotemporal relationship between gaze and hand positions, we computed the cross-correlation between gaze and hand position using an entire series of eight pegs within a specific task phase after downsampling the hand data to 30 Hz to match the sample rate of the gaze data. In particular, we were interested in computing the lag (temporal offset) between the gaze and hand position time series. Temporal offset was modeled with the following equation:

$$\text{Offset} = \text{Block} * \text{Hand} * \text{Phase} + (1 + \text{Block} * \text{Hand} * \text{Phase}|\text{Subject}).$$

From all models, we simplified the fixed effects, random effects, or both to fit the most comprehensive model that still converged. The final form of the model for each analysis is described in the code provided as Extended Data.

Code accessibility. The code/software described in the paper is freely available online at https://github.com/YauLab/NumbPeg (Extended Data 1).

Results

Digital anesthesia alters action durations and force production

We briefly summarize the effects of digital anesthesia on performance during a dexterous motor task (for summarized description of task, see Fig. 1) before presenting the results related to the gaze–hand position relationship, the primary focus of our study. The task was split into two phases: placement or retrieval of pegs. Within each phase, we defined four actions using the force signals measured at the collection trays and pegboard: peg-free hand movement, peg collection, peg transport, and peg delivery. This delineation allowed us to analyze the actions of the tasks in terms of the precision required: coarse collection and delivery involving the collection trays or precise collection and delivery involving the pegboard.

In Experiments 1 and 2, we found that digital anesthesia systematically and reliably altered performance on the dexterous motor task (Extended Data). While participants successfully completed all actions in the placement phase (Extended Data Figs. 2-1, 2-2, 4-1, 4-2) and retrieval phase (Extended Data Figs. 3-1, 3-2, 5-1, 5-2), digital anesthesia resulted in significant changes in the time required to complete the actions and the forces produced by the actions. These results reveal that the acute loss of somatosensory feedback slows motor performance and the capacity to regulate force, consistent with previous studies in deafferented patients (Cuadra et al., 2019). Importantly, saline injections did not induce the same behavioral changes (Extended Data Figs. 4-1, 4-2, 5-1, 5-2), indicating that the altered performance was specifically attributable to the loss of tactile sensation.

Experiment 1: anesthesia modulates eye–hand coordination over phases

We first sought to determine how the loss of sensory feedback on the hand-modulated eye–hand coordination at the level of series which comprised placement and retrieval phases. Given the cyclical nature of the actions within a phase (sequential engagement of eight pegs), we reasoned that the temporal offset computed through cross-correlation analysis would provide a metric capturing the relationship between the gaze and hand positions within a phase. We compared the temporal offset metrics computed from each phase completed before (B1) and after digital anesthesia (B2) to determine the general modulatory effects associated with the loss of sensation. Without anesthesia, gaze position routinely preceded that of the hand in the placement phase (158.7 31.8 ms), consistent with the guidance role of vision. With anesthesia, the offset between the gaze and hand was substantially smaller (73.3 ± 31.8 ms). A model accounted for these patterns with a significant block * hand interaction ($X_1^2 = 8.0$; $p = 0.005$). Post hoc tests revealed that the change in offset for the treated hand differed significantly from the change in offset for the untreated hand ($\Delta\Delta\text{offset} = 58 \pm 21.2$ ms; $t_{(788)} = 2.7$; $p = 0.006$). Notably, anesthesia did not similarly modulate the gaze–hand relationship in the retrieval phase ($\Delta\Delta\text{offset} = 26.7 \pm 21.2$ ms; $t_{(788)} = 1.3$, $p = 0.2$). The absence of an effect in the retrieval phase may be related to the different gaze demands compared with the placement phase. To address this possibility, we next characterized gaze–hand relationships during each action.

Experiment 1: eye–hand coordination in the placement phase is altered by digital anesthesia

Having demonstrated that digital anesthesia modulated performance times and forces generated in the pegboard task, we focused on how somatosensory feedback loss impacted the spatiotemporal relationship between participants' gaze and hand positions during the task. When grasping and transporting objects with intact senses, vision serves primarily to guide planning of subsequent hand movements (Johansson et al., 2001), so gaze position typically leads hand position in space. In this mode, somatosensory signals provide feedback regarding the physical interactions between the hand and grasped object (Johansson and Flanagan, 2009). In the context of our pegboard task, somatosensory feedback would signal the forces applied during peg collection, successful peg grasping and delivery, and stable peg handling during

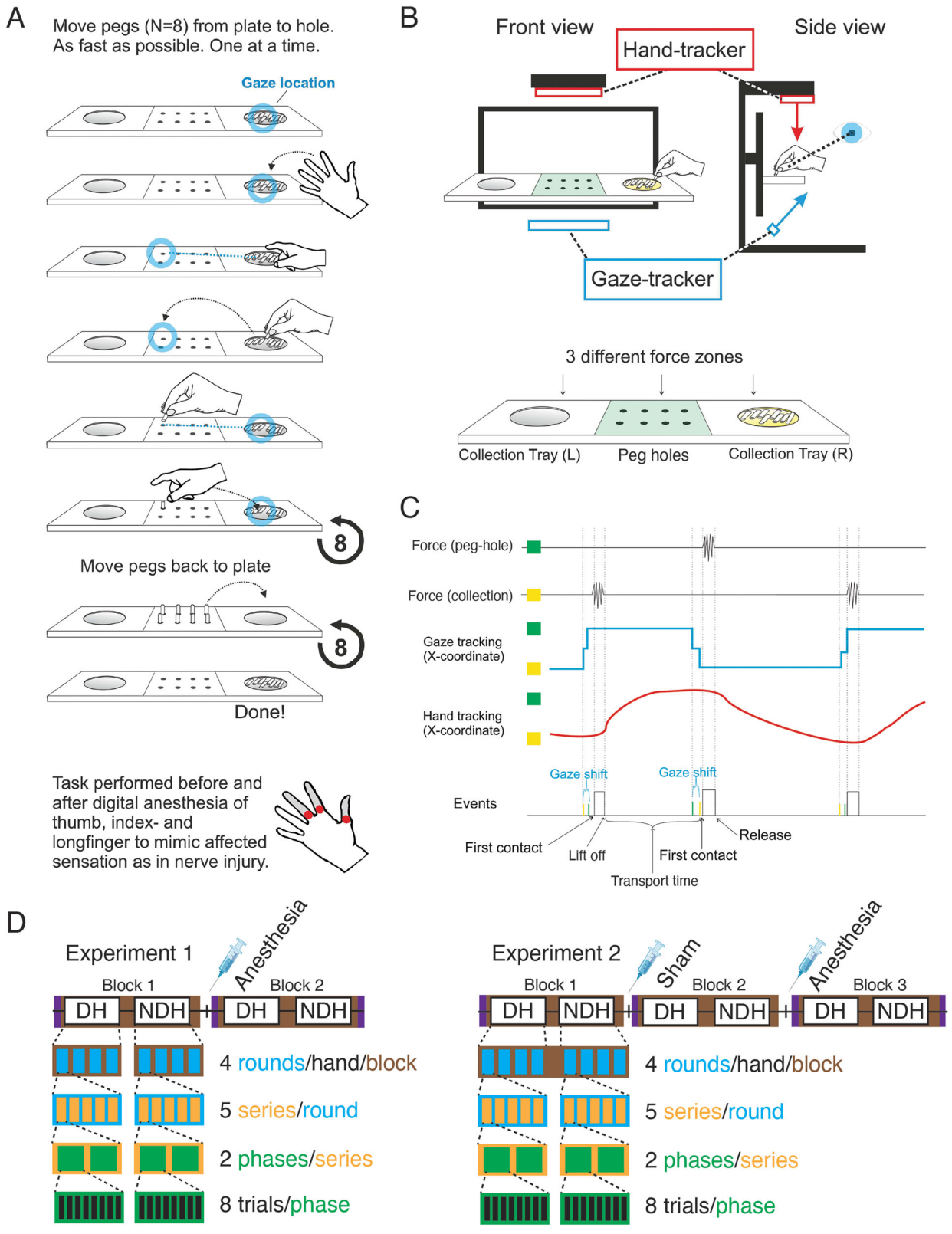

Figure 1. Overview of the workspace, task, and recorded data. ***A***, Schematic of the manual dexterity task. Participants collect an individual peg from the collection tray and deliver the pegs to isolated holes in the delivery tray. This action is performed sequentially for all eight pegs. Each tray has force transducers collecting normal and torque forces. ***B***, Layout of the positioning for the hand tracker, gaze tracker, and pegboard. ***C***, Example traces of the force tracking, hand tracking, and eye tracking during the task. ***D***, Schematic depicting the task structure in Experiment 1 (left) and Experiment 2 (right). Each white box represents a hand within a block. Black ticks represent injection timepoints. The purple box represents 2PD tests. Within each block, there are

transport. With somatosensory feedback loss, we hypothesized that vision would be recruited to provide substitute feedback about the interactions between the hand and grasped object. Accordingly, we predicted that gaze position would be more closely tied to hand position after digital anesthesia.

Having split the task into placement and retrieval phases, we further subdivided the actions within each phase to collection and delivery of the peg (Fig. 2*A*) which involved physical interactions with the tray and pegboard. The phases also comprised movement actions—peg-free hand movement and peg transport—directly preceding the peg collection and delivery actions, respectively. We first examined GISI (see Materials and Methods) at the time of peak normal force production during peg collection, reasoning that participants were maximally engaged with the pegs at this time. A model revealed a significant block * hand interaction ($X_1^2 = 187.7$; $p < 10^{-16}$). Post hoc tests (Fig. 2*B*) revealed a significant decrease in GISI (ΔGISI) after digital anesthesia within the treated hand (ΔGISI = −57.6 ± 3.7 mm; $z = -15.7$; $p < 0.0001$). A comparison between ΔGISI for the treated and untreated hands also revealed significant differences (ΔΔGISI = −70.6 ± 5.2 mm; $z = -13.7$; $p < 0.0001$). Given that the time of peak normal force varied across trials throughout coarse collection, we additionally modeled GISI as a function of progress through coarse collection (Fig. 2*C*). GISI increased monotonically through the action for the untreated hand in B1 and B2. GISI similarly increased monotonically through the action for the treated hand in B1 but remained constant following anesthesia treatment in B2. The model captured these patterns as a significant block * hand * progress interaction ($X_4^2 = 178.2$; $p < 10^{-16}$). Post hoc tests captured the increasing across-hand differences in ΔGISI through the action (onset, ΔΔGISI = −39.6 ± 19.0 mm; $z = -2.1$; $p = 0.04$; AP_{25}, ΔΔGISI = −44.4 ± 19.0 mm; $z = -2.3$; $p = 0.02$; AP_{50}, ΔΔGISI = −62.9 ± 19.0 mm; $z = -3.3$; $p = 0.001$; AP_{75}, ΔΔGISI = −90.0 ± 19.0 mm; $z = -4.7$; $p < 0.0001$; offset, ΔΔGISI = −112.1 ± 19.0 mm; $z = -5.9$; $p < 0.0001$). These data suggest that participants were typically less reliant on gaze to accomplish coarse collection and quicker to look ahead to the next location in control conditions. In contrast, participants looked closer at their hands and maintained this gaze–hand relationship during coarse collection following the loss of somatosensory feedback.

Given the adaptations of eye–hand coordination when interacting with a peg, we next asked whether these adjustments also occur in actions that did not involve peg manipulation. We examined gaze–hand position relationships during all peg-free hand movement actions leading up to coarse collection (Fig. 2*D*; i.e., hand movements after peg delivery and prior to peg collection). Given that nothing was held in the hand during this action, we did not predict differences in gaze–hand relationship related to anesthesia for these events. Contrary to our prediction, a model revealed a significant block * hand * progress interaction ($X_4^2 = 27.1$; $p = 10^{-5}$; Fig. 2*D*). Post hoc tests revealed significant differences in ΔGISI for the treated and untreated hands throughout the movement action (onset, ΔΔGISI = −36.8 ± 5.1 mm; $z = -7.2$; $p < 0.001$; AP_{25}, ΔΔGISI = −45.8 ± 5.1 mm; $z = -9.0$; $p < 0.0001$; AP_{50}, ΔΔGISI = −11.4 ± 5.1 mm; $z = -2.2$; $p = 0.02$; AP_{75}, ΔΔGISI = −38.8 ± 5.1 mm; $z = -7.6$; $p < 0.0001$; offset, ΔΔGISI = −38.6 ± 5.1 mm; $z = -7.6$; $p < 0.0001$). These results indicated that the reduced separation in gaze–hand position during the anesthesia condition was maintained throughout the hand movement action. The fact that gaze was more closely anchored to the hand during peg-free hand movements indicates that the compensatory changes in eye–hand coordination are not specific to hand actions involving object manipulation.

We then examined gaze–hand position relationships during precise delivery when participants were tasked with placing the peg into a small hole on the pegboard. We reasoned that this action required more precision and a higher degree of eye–hand coordination compared with the other actions even with intact somatosensation. Accordingly, we predicted that gaze–hand relationships would be relatively unchanged comparing B2 and B1 for both hands. Consistent with our prediction, the block * hand interaction failed to reach significance ($X_1^2 = 0.29$; $p = 0.59$) for GISI differences at the time of peak normal force production (Fig. 2*E*). Visual inspection of GISI dynamics over the delivery action (Fig. 2*F*) indicated subtle differences between the treated and untreated hands: GISI increased at the end of the delivery action with both hands prior to treatment and with the untreated hand in B2, while GISI remained low with the anesthetized hand. These patterns were captured by a significant block * hand * progress interaction ($X_4^2 = 113.0$; $p < 10^{-16}$), driven by ΔGISI difference between treated and untreated hands only during the end of the delivery action (ΔΔGISI = −29.9 ± 9.2 mm; $z = -3.3$; $p = 0.001$). These results revealed that performance of precise delivery under all conditions required gaze recruitment; however, gaze position was released more quickly following peg delivery in conditions with reliable somatosensation compared with the anesthesia condition. The loss of somatosensory feedback appeared to increase participants' reliance on vision to complete precise peg delivery.

Lastly, we examined gaze–hand position relationships during peg transport leading to precise delivery (Fig. 2*G*). At the start of this transport action, participants look toward the pegboard while they maintain their hold on the peg with intact somatosensation resulting in a relatively large GISI. In the anesthesia condition, participants fixed their gaze on their hand, resulting in a small GISI that remained relatively unchanged throughout the action. A model accounted for these patterns with a significant block * hand * progress interaction ($X_4^2 = 1{,}133.6$; $p < 10^{-16}$). Post hoc tests revealed significant hand differences at the onset of the transport action (ΔΔGISI = −109.7 ± 9.8 mm; $z = -11.2$; $p < 0.0001$) and the first half of the

←

four rounds (teal) of data collection where each round contains five series (orange) with two phases (green). The placement phase comprised eight pegs (black) collected and delivered sequentially followed by the retrieval phase, totaling 160 peg placements and 160 peg retrievals per hand per block. DH, dominant hand; NDH, nondominant hand.

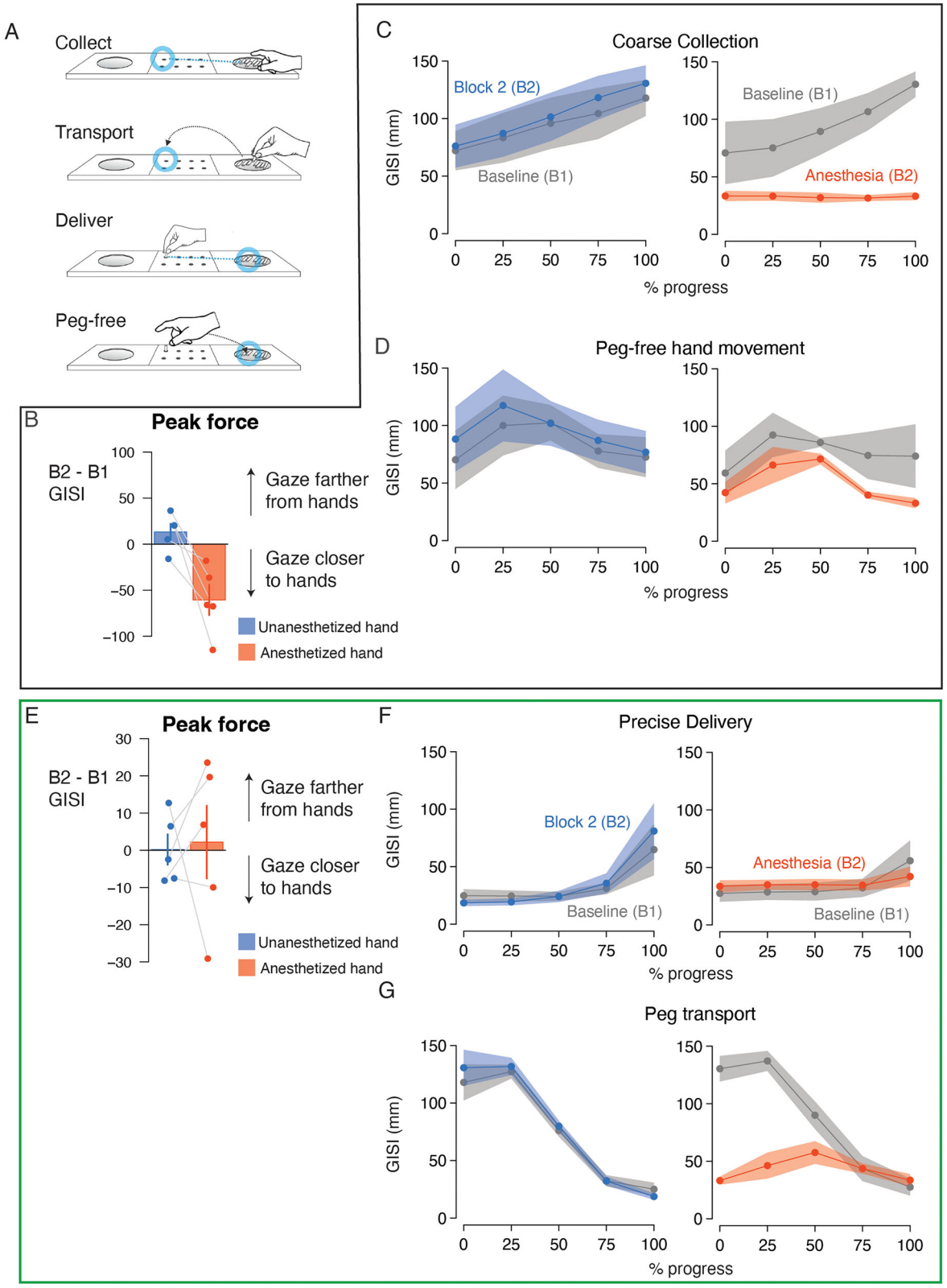

Figure 2. Experiment 1: gaze more closely tracked the hands in the placement phase following anesthesia treatment. ***A***, Schematic of the task during the placement phase in Experiment 1 divided into the constitutive actions. ***B***, Bar plots showing the mean change in GISI at peak force during coarse collection between Block 1 (preanesthesia) and Block 2 (postanesthesia) with the dominant (blue) and nondominant (red) hands. The error bar indicates SEM. Connected markers indicate data from individual participants. ***C***, Lines and markers indicate mean GISI (average of participant-level means) calculated as a function of progress (%) through the coarse collection action with the dominant hand (left plot) and nondominant hand (right plot). The shaded region indicate SEM. Gray data indicate GISI in the baseline blocks. Blue data indicate GISI for the dominant hand (control) in Block 2. Red data indicate GISI for

transport action (AP_{25}, $\Delta\Delta GISI = -94.8 \pm 9.8$ mm; $z = -9.7$; $p < 0.0001$; AP_{50}, $\Delta\Delta GISI = -35.5 \pm 9.8$ mm; $z = -3.6$; $p = 0.0003$). Together, these results support our hypothesis that vision, which typically precedes and guides hand movements, was recruited to monitor the status of the grasped peg during transport following somatosensory feedback loss.

In sum, these analyses revealed the effect of digital anesthesia on eye–hand coordination during collection, transport, and delivery actions during the placement phase: Gaze tracked more closely with the hand following the loss of somatosensory feedback. GISI changes related to digital anesthesia were obvious during coarse collection and peg transport events, implying that vision was recruited to support feedback mechanisms typically governed by touch. GISI modulation during precise delivery may be more subtle because this action typically required more visual support. Notably, the closer gaze–hand relationship during peg-free hand movements suggests a general compensatory mechanism in which vision becomes spatially yoked to the hand even in the absence of object manipulation.

Experiment 1: eye–hand coordination in the retrieval phase is altered by digital anesthesia

To address whether the changes in gaze–hand coordination were context dependent, we also analyzed gaze–hand relationships during the retrieval phase of the task, where peg collection required more precision and peg delivery was coarser than in the placement phase (Fig. 3*A*). Analysis of the peg-free hand movement and transport actions additionally enabled us to evaluate whether gaze–hand compensatory changes extended to movement actions and required peg manipulation.

To quantify eye–hand coordination during precise collection, we first evaluated gaze–hand relationships when participants produced the maximum force on the pegboard (Fig. 3*B*). A model captured a modest but significant reduction in ΔGISI during peak force application in the treated hand compared with the untreated hand with a block * hand interaction ($X^2_1 = 10.1$; $p = 0.002$; $\Delta\Delta GISI = -14.4 \pm 4.5$ mm; $z = -3.2$; $p = 0.002$). Across the precise collection action (Fig. 3*C*), GISI for both hands during B1 and B2 initially exhibited similar increases; however, the separation between the gaze and anesthetized hand leveled off during the second half of the collection action, while the separation continued to grow in the other conditions. The model accounted for this pattern with a significant block * hand * progress interaction ($X^2_4 = 24.5$; $p = 10^{-5}$). Although ΔΔGISI did not differ significantly in any specific action quartile, ΔGISI for the treated hand tended to be larger than that for the untreated hand at the end of the precise collection ($\Delta\Delta GISI = -23.0 \pm 14.1$ mm). A potential explanation for the more subtle anesthesia effects on precise collection may be that this action required more gaze involvement even with intact somatosensation. Indeed, GISI values during precise collection (56.2 ± 4.4 mm) were significantly lower ($t_{(30.9)} = 2.6$; $p = 0.01$) compared with GISI values during coarse collection (78.8 ± 7.4 mm; Fig. 2*C*).

The peg-free hand movement actions in retrieval phases were generally characterized by an initial large separation in gaze–hand position that decreased over the movement action (Fig. 3*D*). This pattern is consistent with the notion that precise collection is a visually guided process in which participants initially direct their gaze to the pegboard to localize the target peg before they subsequently moved their hand to retrieve the peg. Although visual inspection of the data revealed that gaze and hand positions converge at the pegboard in all conditions, a smaller separation between participants' gaze and their anesthetized hands during the early portion of the movement action was also apparent. These patterns were captured by a significant block * hand * progress interaction ($X^2_4 = 103.1$; $p < 10^{-16}$). Post hoc tests revealed significant differences between the treated and untreated hand during the initial movement intervals (onset, $\Delta\Delta GISI = -37.6 \pm 8.2$ mm; $z = -4.6$; $p < 0.0001$; AP_{25}, $\Delta\Delta GISI = -27.27 \pm 8.2$ mm; $z = -3.3$; $p = 0.0009$). These results indicate that participants directed their gaze closer to their hands following the loss of somatosensory feedback during hand movements preceding precise collection, consistent with the results in the peg-free hand movement action during coarse collection. These results were inconsistent with the hypothesis of a compensatory eye–hand coordination process being event-specific and dependent on interactions with objects.

We next compared gaze–hand position relationship during coarse delivery. During peak force production, ΔGISI differed significantly between the treated and untreated hand (block * hand interaction, $X^2_1 = 99.5$; $p < 10^{-16}$; Fig. 3*E*). Over the duration of the coarse delivery action (Fig. 3*F*), GISI tended to be relatively stable with a minor increase in all conditions; however, GISI was notably lower for the treated hand in B2. Accordingly, a model revealed a significant block * hand interaction ($X^2_1 = 506.9$; $p < 10^{-16}$), but the block * hand * progress interaction ($X^2_4 = 3.5$, $p = 0.48$) failed to achieve significance. The post hoc test on the block * hand interaction confirmed that ΔGISI for the anesthetized hand was significantly lower compared with the nonanesthetized hand throughout coarse delivery ($\Delta\Delta GISI = 43.7 \pm 1.9$ mm; $z = 22.5$; $p < 0.0001$). These results demonstrate that vision was recruited to compensate for the loss of somatosensory feedback when participants returned the pegs to the large trays.

Lastly, we evaluated anesthesia effects on gaze–hand relationships during peg transport preceding coarse delivery. Given our hypothesis that vision is recruited to provide object manipulation feedback when touch is lost, we predicted

←

the nondominant (anesthetized) hand in Block 2. ***D***, Lines and markers indicate mean GISI calculated as a function of progress (%) through the peg-free hand movement action. Conventions as in ***C***. ***E***, Bar plots showing the mean change in GISI at peak force during precise delivery. Conventions as in ***B***. ***F***, Lines and markers indicate mean GISI calculated as a function of progress (%) through the precise delivery action. Conventions as in ***C***. ***G***, Lines and markers indicate mean GISI calculated as a function of progress (%) through the peg transport action. Conventions as in ***C***. Force data for the placement phase of Experiment 1 is shown in Extended Data Figure 2-1. Summary statistics are provided in Extended Data Figure 2-2. Statistics of potential learning effects are provided in Extended Data Figure 2-3.

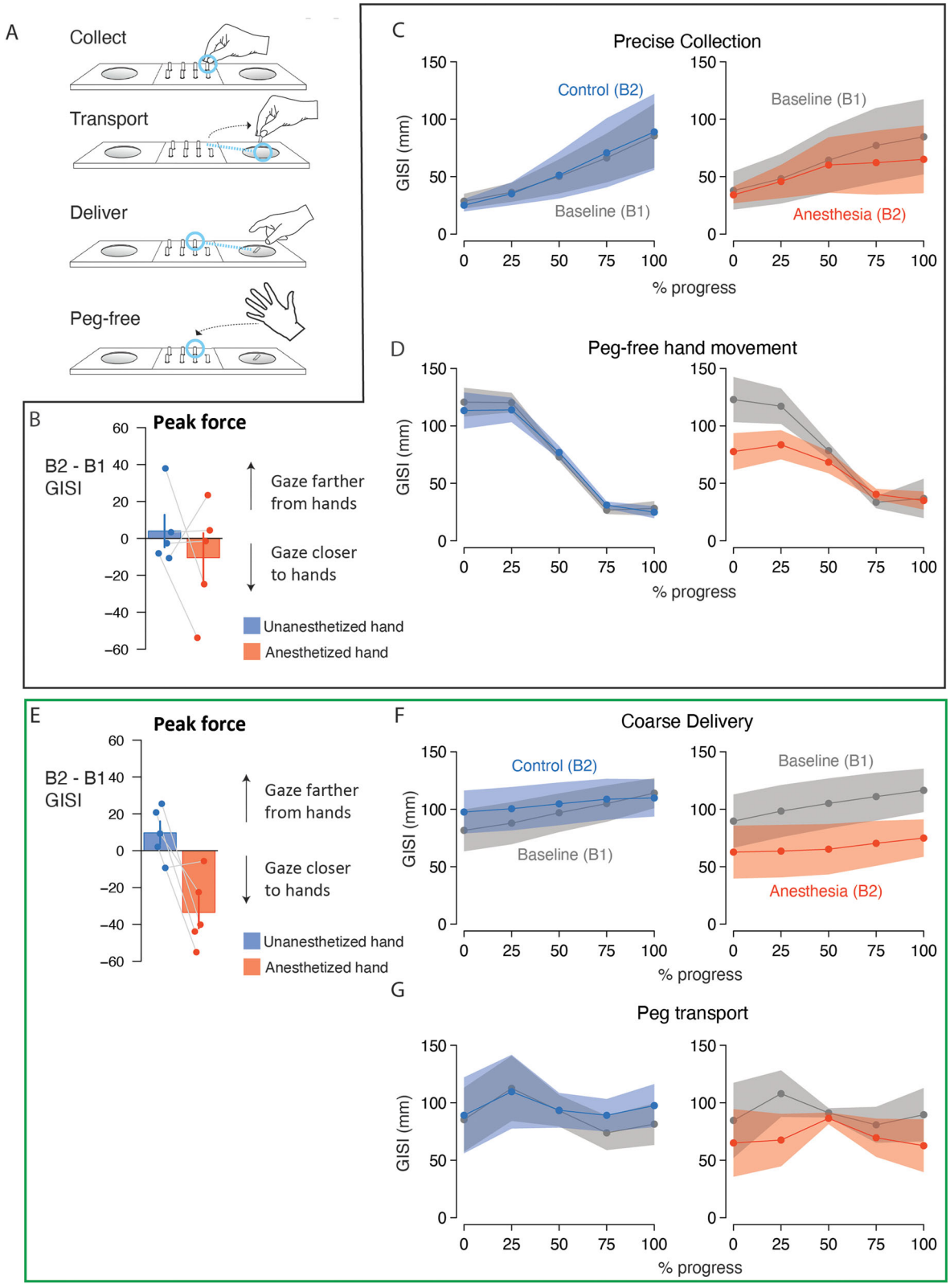

Figure 3. Experiment 1: gaze more closely tracked the hands in the retrieval phase after anesthesia treatment. ***A***, Schematic of the task during the retrieval phase in Experiment 1 divided into the constitutive actions. ***B***, Bar plots showing the mean change in GISI at peak force during precise collection between Block 1 (preanesthesia) and Block 2 (postanesthesia) with the dominant (blue) and nondominant (red) hands. The error bar indicate SEM. Connected markers indicate data from individual participants. ***C***, Lines and markers indicate mean GISI (average of participant-level means) calculated as a function of progress (%) through the precise collection action with the dominant hand (left plot) and nondominant hand (right plot). The shaded region indicates SEM. Gray data indicate GISI in the baseline blocks. Blue data indicate GISI for the dominant hand (control) in Block 2. Red data indicate GISI for the

that gaze would be more closely tied to the hand during peg transport with digital anesthesia compared with conditions with intact touch. Consistent with this prediction, we observed reduced separation between participants' gaze and the anesthetized hand (Fig. 3*G*). This pattern was captured by a significant block * hand * progress interaction ($X^2_4 = 35.1$; $p = 10^{-7}$). Post hoc tests revealed significant ΔΔGISI differences early and late in the transport action (onset, ΔΔGISI = −23.5 ± 8.6 mm; $z = -2.7$; $p = 0.006$; AP_{25}, ΔΔGISI = −37.9 ± 8.6 mm; $z = -4.4$; $p < 0.0001$; AP_{75}, ΔΔGISI = −26.1 ± 8.6 mm; $z = -3.0$; $p = 0.002$; offset, ΔΔGISI = −42.4 ± 8.6 mm; $z = -4.9$; $p < 0.0001$). These collective results indicate a tighter gaze–hand relationship during peg transport following somatosensory feedback loss.

Experiment 2: anesthesia modulates eye–hand coordination over phases

In Experiment 1, the nondominant hand received digital anesthesia in all participants. Moreover, behavior with the anesthetized hand was compared only against behavior with the untreated, dominant hand. Accordingly, the task performance and gaze behavior changes could be attributable simply to an increased salience of the nondominant hand because it received an injection rather than reflecting the loss of sensation on that hand. To address this potential confound, we performed a second experiment with a new group of participants. In Experiment 2, participants performed the pegboard task with their dominant hand under three conditions: no treatment (B1), injection with saline (B2), and injection with anesthesia (B3). The nondominant hand was tested during B1, B2, and B3 without treatment to account for the passage of time and potential learning effects. This design explicitly (1) accounts for hand dominance (comparing with Experiment 1), (2) provides an internal control (comparing sham vs anesthesia in Experiment 2), and controls for block (comparing Experiment 1 anesthesia condition with Experiment 2 sham condition).

Just as we did for Experiment 1, we first assessed whether anesthesia modulated gaze–hand relationships at the temporal scale of phases. Consistent with Experiment 1 results, smaller offsets were observed for the anesthetized hand compared with the other conditions. A model captured this effect with a significant block * hand interaction ($X^2_2 = 25.4$; $p = 10^{-6}$). Post hoc tests revealed that the offset change for the treated hand differed significantly from the offset change for the untreated hand (ΔΔoffset = 100.0 ± 21.6 ms; $t = 4.6$; $p < 0.0001$). In contrast, anesthesia did not significantly modulate gaze–hand relationships during the retrieval phase (ΔΔoffset = 31.67 ± 21.6 ms; $t = 1.5$; $p = 0.31$). These collective results are consistent with the offset results in Experiment 1.

Experiment 2: eye–hand coordination in the placement phase is altered by digital anesthesia

During the coarse collection action (Fig. 4), we found a significant block * hand interaction on the separation of the gaze and hand at the time of peak force production ($X^2_2 = 124.5$; $p < 10^{-16}$) contrasting the results from testing after sham injection (B2) compared with testing after anesthesia injection (B3). A post hoc test (Fig. 4*B*) revealed that the B3–B2 difference (ΔGISI) with the dominant (treated) hand was significantly larger than the difference with the nondominant hand (ΔΔGISI = 51.4 ± 7.8 mm; $z = 10.7$; $p < 0.0001$). Considering how gaze–hand separation varied over the coarse collection action (Fig. 4*C*), we observed that the separation increased monotonically through the action when testing with intact sensation for both hand testing (i.e., during B1 and B2). Notably, the gaze–hand separation remained relatively constant during the action with digital anesthesia, suggesting that gaze position was relatively fixed on hand position (Fig. 4*C*, right). These patterns were captured by a significant block * hand * progress interaction ($X^2_8 = 433.12$; $p < 10^{-16}$). Post hoc tests revealed significant gaze–hand separation differences comparing the treated hand during B3 compared with B1 (AP_{50}, ΔΔGISI = −28.1 ± 4.5 mm; $z = -6.2$; $p < 0.0001$; AP_{75}, ΔΔGISI = −65.7 ± 4.5 mm; $z = -14.5$; $p < 0.0001$; offset, ΔΔGISI = −100.0 ± 4.5 mm; $z = -22.1$; $p < 0.0001$) and B2 (onset, ΔΔGISI = −23.2 ± 4.5 mm; $z = -5.1$; $p < 0.0001$; AP_{25}, ΔΔGISI = −28.0 ± 4.5 mm; $z = -6.2$; $p < 0.0001$; AP_{50}, ΔΔGISI = −39.1 ± 4.5 mm; $z = -8.6$; $p < 0.0001$; AP_{75}, ΔΔGISI = −65.1 ± 4.5 mm; $z = -14.4$; $p < 0.0001$; offset, ΔΔGISI = −100.0 ± 4.5 mm; $z = -21.0$; $p < 0.0001$) for most progress points. Notably, a block * hand interaction ($X^2_2 = 654.6$; $p < 10^{-16}$) and follow-up post hoc analysis also revealed modest but significant gaze–hand coordination changes after sham injection (B2–B1; ΔΔGISI = 13.6 ± 2.0 mm; $z = 6.7$; $p < 0.0001$) but with increased gaze–hand separation compared with the no injection condition. Accordingly, the dramatic reduction in gaze–hand separation following digital anesthesia occurred despite the effects observed from the sham intervention. These anesthesia results are consistent with the coarse collection results in Experiment 1.

Peg-free hand movement in the placement phase also exhibited changes in eye–hand coordination after anesthesia (Fig. 4*D*). With intact sensation, the gaze and hand positions were characterized by an initially large separation that decreased as they converged on the collection tray. In contrast, the gaze and hand positions remained in closer proximity throughout the movement action after the treated hand was anesthetized. A model accounted for this pattern with a significant block * hand * progress interaction ($X^2_8 = 254.8$; $p < 10^{-16}$). Post hoc tests revealed that the differences in

←

nondominant (anesthetized) hand in Block 2. ***D***, Lines and markers indicate mean GISI calculated as a function of progress (%) through the peg transport action. Conventions as in ***C***. ***E***, Bar plots showing the mean change in GISI at peak force during coarse delivery. Conventions as in ***B***. ***F***, Lines and markers indicate mean GISI calculated as a function of progress (%) through the coarse delivery action. Conventions as in ***C***. ***G***, Lines and markers indicate mean GISI calculated as a function of progress (%) through the peg transport action. Conventions as in ***C***. Force data for the retrieval phase of Experiment 1 are shown in Extended Data Figure 3-1. Summary statistics are provided in Extended Data Figure 3-2. Statistics of potential learning effects are provided in Extended Data Figure 3-3.

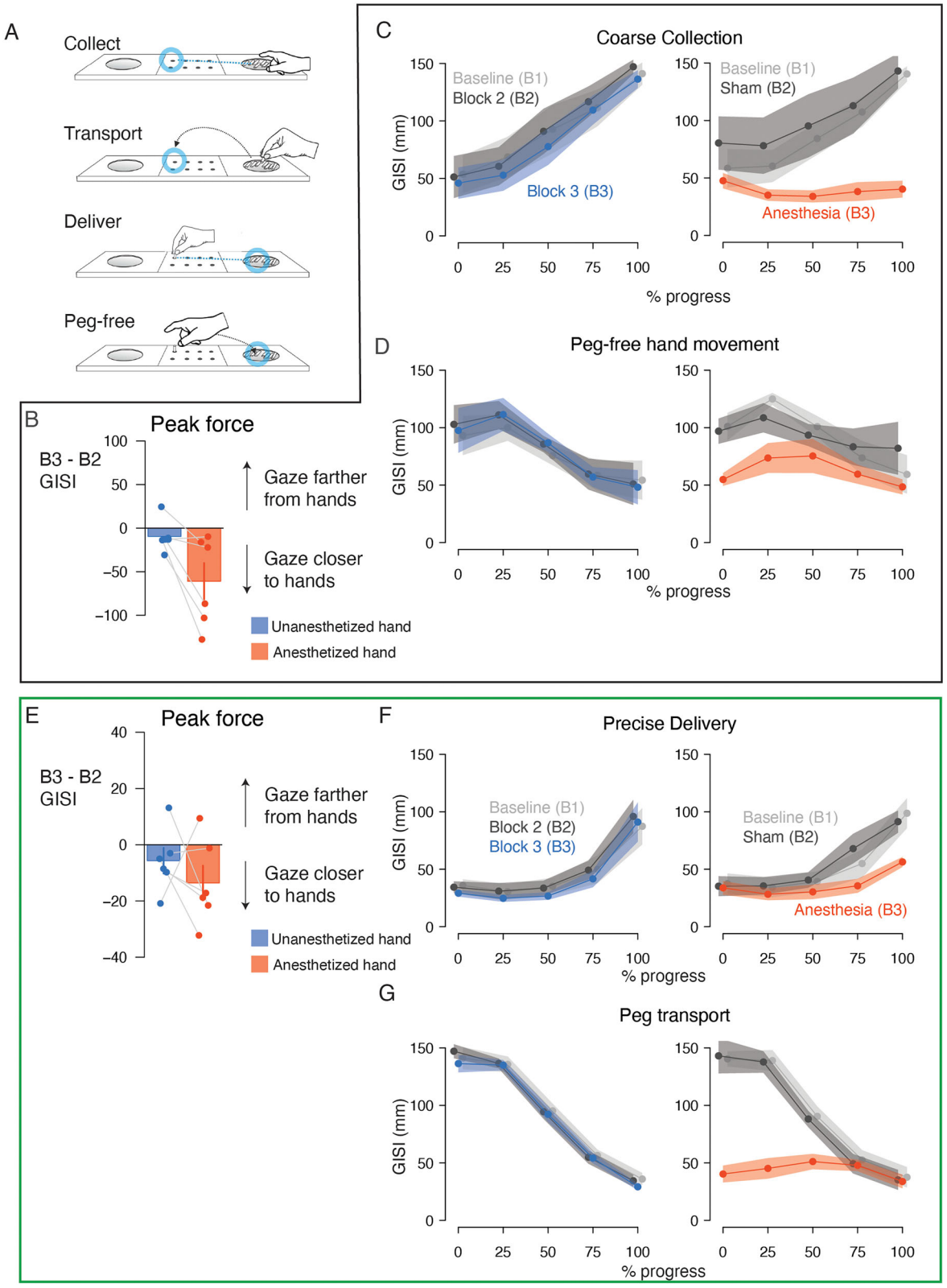

Figure 4. Experiment 2: gaze more closely tracked the hands in the placement phase following anesthesia treatment. ***A***, Schematic of the task during the placement phase in Experiment 2 divided into the constitutive actions. ***B***, Bar plots showing the mean change in GISI at peak force during coarse collection between Block 2 (sham) and Block 3 (postanesthesia) with the nondominant (blue) and dominant (red) hands. The error bar indicates SEM. Connected markers indicate data from individual participants. ***C***, Lines and markers indicate mean GISI (average of participant-level means) calculated as a function of progress (%) through the coarse collection action with the nondominant hand (left plot) and dominant hand (right plot). The shaded region indicates SEM. Light gray data indicate GISI in the baseline blocks. Dark gray data indicate GISI in Block 2 for the nondominant hand and dominant hand (sham). Blue data

gaze–hand separation measured for the treated hand after anesthesia compared with sham were significantly greater than the corresponding ΔGISI values for the untreated hand during all quartiles (onset, ΔΔGISI = −46.2 ± 4.5 mm; $z = -10.4$; $p < 0.0001$; AP_{25}, ΔΔGISI = −53.0 ± 4.5 mm; $z = -11.9$; $p < 0.0001$; AP_{50}, ΔΔGISI = −32.3 ± 4.5 mm; $z = -7.3$; $p < 0.0001$; AP_{75}, ΔΔGISI = −25.3 ± 4.5 mm; $z = -5.7$; $p < 0.0001$; offset, ΔΔGISI = −25.3 ± 4.5 mm; $z = -5.7$; $p < 0.0001$). Similarly, differences in gaze–hand separation measured for the treated hand after anesthesia compared with baseline were significantly greater than the corresponding ΔGISI values for the untreated hand during all quartiles (onset, ΔΔGISI = −56.9 ± 4.5 mm; $z = -12.8$; $p < 0.0001$; AP_{25}, ΔΔGISI = −73.3 ± 4.5 mm; $z = -16.5$; $p < 0.0001$; AP_{50}, ΔΔGISI = −44.6 ± 4.5 mm; $z = -10.0$; $p < 0.0001$). Importantly, ΔGISI did not differ between the treated and untreated hands comparing sham against the baseline times (ΔΔGISI = 1.9 ± 2.0 mm; $z = 0.9$; $p = 0.62$). These results are consistent with the peg-free hand movement results in Experiment 1.

Following coarse collection, the pegs are transported and delivered to the pegboard. The separation between the gaze and hand at the time of peak force application during peg delivery (Fig. 4*E*) significantly differed between the treated and untreated hand (ΔΔGISI = −9.01 ± 3.5 mm, $z = -2.6$; $p = 0.03$) when comparing B1 and B3 (block * hand interaction; $X_2^2 = 7.9$; $p = 0.03$). With intact sensation, gaze and hand positions remain in close proximity during the initial course of precise delivery before gaze is released; however, GISI values for the anesthetized hand remain low for a more extensive portion of the action. These patterns (Fig. 4*F*) are captured by a significant a block * hand interaction ($X_2^2 = 123.0$; $p < 10^{-16}$) and a block * hand * progress interaction ($X_8^2 = 182.3$; $p < 10^{-16}$). Post hoc tests indicated that ΔGISI in the early AP was statistically indistinguishable between the treated and untreated hand. Importantly, post hoc across-hand comparisons revealed significant differences during the end of the precise delivery action comparing anesthesia to sham (B3–B2; offset, ΔΔGISI = −38.4 ± 3.8 mm; $z = -10.263$; $p < 0.0001$) and comparing anesthesia to baseline (B3–B1; offset, ΔΔGISI = −51.3 ± 3.75 mm; $z = -13.8$; $p < 0.0001$). These anesthesia effects occurred despite subtle sham effects (B2–B1; ΔΔGISI = 5.1 ± 1.7 mm; $z = 3.0$; $p = 0.007$) which were associated with gaze–hand separation increases. The anesthesia results are consistent with the precise placement results in Experiment 1.

Lastly, we evaluated gaze–hand relationships during peg transport (Fig. 4*G*). With intact sensation, the separation between gaze and hand positions was high at the beginning of transport, presumably reflecting a tendency for participants to look at the pegboard in advance of peg transport and the eventual convergence of gaze and hand positions. In contrast, gaze–hand separation was lower and relatively constant with the anesthetized hand. The model accounted for these patterns with a significant block * hand * progress interaction ($X_8^2 = 1{,}089.6$; $p < 10^{-16}$). Post hoc tests revealed significant ΔGISI differences between the treated and untreated hands during the initial three progress portions contrasting anesthesia and sham (B3–B2; onset, ΔΔGISI = −95.1 ± 3.4 mm; $z = -27.7$; $p < 0.0001$; AP_{25}, ΔΔGISI = −94.9 ± 3.4 mm; $z = -27.6$; $p < 0.0001$; AP_{50}, ΔΔGISI = −38.0 ± 3.4 mm; $z = -11.0$; $p < 0.0001$) and anesthesia and baseline (B3–B1; onset, ΔΔGISI = −100.0 ± 3.4 mm; $z = -29.1$; $p < 0.0001$; AP_{25}, ΔΔGISI = −91.7 ± 3.4 mm; $z = -26.7$; $p < 0.0001$; AP_{50}, ΔΔGISI = −33.1 ± 3.4 mm; $z = -9.6$; $p < 0.0001$). No hand differences were observed contrasting sham and baseline (B2–B1; ΔΔGISI = 1.5 ± 1.5 mm; $z = 0.9$; $p = 0.61$). These results are consistent with the peg transport results in Experiment 1.

Experiment 2: eye–hand coordination in the retrieval phase is altered by digital anesthesia

To examine how anesthesia influenced gaze–hand coordination while accounting for hand dominance and sham effects, we additionally analyzed data collected during peg-free hand movement, precise collection, transport, and coarse delivery in the retrieval phase (Fig. 5*A*).

At peak force application during precise collection, we found that the gaze–hand separation for the treated and untreated hands changed differentially between the B2 (sham) and B3 (anesthesia) blocks (Fig. 5*B*; block * hand interaction; $X_2^2 = 128.4$; $p < 10^{-16}$). A post hoc test confirmed that the change in GISI (sham vs anesthesia) for the treated hand differed significantly from the change in GISI for the untreated hand over the corresponding blocks (ΔΔGISI = −50.79 ± 4.75 mm; $z = -10.7$; $p < 0.0001$). The effect of anesthesia was also evident over the entire collection action (Fig. 5*C*); GISI steadily increased in the baseline and control conditions, while it remained low in the anesthesia condition. These patterns were captured by a significant block * hand * progress interaction ($X_8^2 = 232.8$; $p < 10^{-16}$). The across-hand differences in ΔGISI was significant in all action portions comparing B3 to B2 (onset, ΔΔGISI = −23.0 ± 5.2 mm; $z = -4.5$; $p < 0.0001$; AP_{25}, ΔΔGISI = −44.5 ± 5.2 mm; $z = -8.6$; $p < 0.0001$; AP_{50}, ΔΔGISI = −71.7 ± 5.2 mm; $z = -13.9$; $p < 0.0001$; AP_{75}, ΔΔGISI = −95.4 ± 5.2 mm; $z = -18.5$; $p < 0.0001$; offset, ΔΔGISI = −95.2 ± 5.2 mm; $z = -18.5$; $p < 0.0001$) and B3 to B1 (onset, ΔΔGISI = −20.3 ± 5.2 mm; $z = -3.9$; $p = 0.0003$; AP_{25}, ΔΔGISI = −33.7 ± 5.2 mm; $z = -6.5$; $p < 0.0001$; AP_{50}, ΔΔGISI = −54.9 ± 5.2 mm; $z = -10.6$; $p < 0.0001$; AP_{75}, ΔΔGISI = −85.8 ± 5.2 mm; $z = -16.6$; $p < 0.0001$; offset, ΔΔGISI = −103.6 ± 5.2 mm; $z = -20.1$; $p < 0.0001$). In contrast, a significant block * hand interaction ($X_2^2 = 996.0$; $p < 10^{-16}$) and

←

indicate GISI for the nondominant hand in Block 3. Red data indicate GISI for the dominant (anesthetized) hand in Block 3. ***D***, Lines and markers indicate mean GISI calculated as a function of progress (%) through the peg-free hand movement action. Conventions as in ***C***. ***E***, Bar plots showing the mean change in GISI at peak force during precise delivery. Conventions as in ***B***. ***F***, Lines and markers indicate mean GISI calculated as a function of progress (%) through the precise delivery action. Conventions as in ***C***. ***G***, Lines and markers indicate mean GISI calculated as a function of progress (%) through the peg transport action. Conventions as in ***C***. Force data for the placement phase of Experiment 2 is shown in Extended Data Figure 4-1. Summary statistics are provided in Extended Data Figure 4-2. Statistics of potential learning effects are provided in Extended Data Figure 4-3.

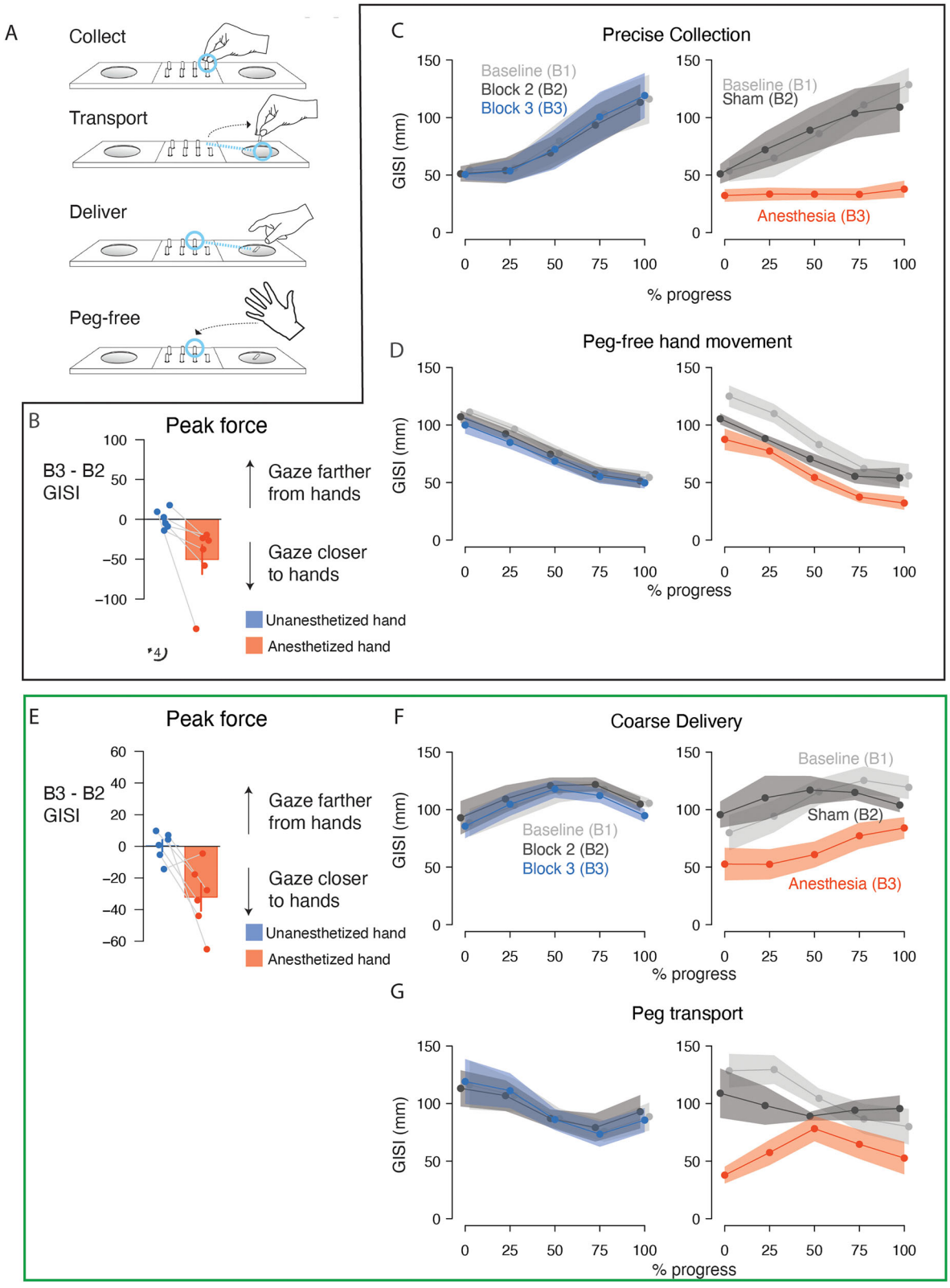

Figure 5. Experiment 2: gaze more closely tracked the hands in the retrieval phase following anesthesia treatment. ***A***, Schematic of the task during the retrieval phase in Experiment 2 divided into the constitutive actions. ***B***, Bar plots showing the mean change in GISI at peak force during precise collection between Block 2 (sham) and Block 3 (postanesthesia) with the nondominant (blue) and dominant (red) hands. The error bar indicate SEM. Connected markers indicate data from individual participants. ***C***, Lines and markers indicate mean GISI (average of participant-level means) calculated as a function of progress (%) through the precise collection action with the nondominant hand (left plot) and dominant hand (right plot). The shaded region indicates SEM. Light gray data indicate GISI in the baseline blocks. Dark gray data indicate GISI in Block 2 for the nondominant hand and dominant hand

subsequent post hoc analyses revealed significant across-hand differences in ΔGISI comparing sham and baseline conditions (B2–B1; $\Delta\Delta GISI_{B2-B1} = 6.3 \pm 2.3$ mm; $z = 2.7$; $p = 0.02$), indicating that gaze–hand separation increased slightly following sham injection. These anesthesia results are consistent with the precise collection results in Experiment 1.

In all conditions, the peg-free hand movement action before precise collection was characterized by a monotonic reduction in the separation between gaze and hand positions (Fig. 5*D*). While there was substantial overlap in the GISI traces for the untreated hand over B1, B2, and B3, the GISI traces for the treated hand exhibited differences with larger values in the sham condition and smaller values in the anesthesia condition. These patterns were captured by a significant block * hand interaction ($X^2_2 = 207.7$; $p = 10^{-16}$). The block * hand * progress interaction achieved significance ($X^2_8 = 15.5$; $p = 0.05$) despite the similar dynamics in all conditions. Post hoc tests revealed significant ΔGISI differences between the treated and untreated hands contrasting B3 to B2 (onset, $\Delta\Delta GISI = -16.5 \pm 3.4$ mm; $z = -4.2$; $p = 0.0001$; AP_{50}, $\Delta\Delta GISI = -15.2 \pm 3.4$ mm; $z = -3.9$; $p = 0.0003$; AP_{75}, $\Delta\Delta GISI = -21.3 \pm 3.4$ mm; $z = -5.4$; $p < 0.0001$; offset, $\Delta\Delta GISI = -25.0 \pm 5.2$ mm; $z = -6.3$; $p < 0.0001$) and to B1 (onset, $\Delta\Delta GISI = -28.7 \pm 3.4$ mm; $z = -7.3$; $p < 0.0001$; AP_{25}, $\Delta\Delta GISI = -22.4 \pm 3.4$ mm; $z = -5.7$; $p < 0.0001$; AP_{50}, $\Delta\Delta GISI = -24.2 \pm 3.4$ mm; $z = -6.2$; $p < 0.0001$; AP_{75}, $\Delta\Delta GISI = -25.3 \pm 3.4$ mm; $z = -6.4$; $p < 0.0001$; offset, $\Delta\Delta GISI = -22.8 \pm 3.4$ mm; $z = -5.8$; $p < 0.0001$). Importantly, across-hand ΔGISI differences were also significant comparing B3 to B2 ($\Delta\Delta GISI = -17.26 \pm 1.8$ mm; $z = -9.8$; $p < 0.0001$), so the loss of sensory feedback with the dominant hand resulted in an even tighter association between spatial association between gaze and hand positions compared with that achieved with the sham injection, which were also significant ($\Delta\Delta GISI = -7.4 \pm 1.8$ mm; $z = -4.2$; $p < 0.0001$). These results are consistent with the peg-free action results in Experiment 1.

Gaze–hand relationships differed significantly at the time of peak force production during coarse delivery (block * hand interaction; $X^2_2 = 69.3$; $p = 10^{-16}$; Fig. 5*E*). Post hoc tests revealed significant differences between ΔGISI contrasting B3 and B2 for the treated and untreated hand ($\Delta\Delta GISI = -32.6 \pm 4.5$ mm; $z = -7.2$; $p < 0.0001$). A tighter spatial relationship between the gaze and anesthetized hand was also evident throughout coarse delivery action in comparison with the other conditions (Fig. 5*F*). A model accounted for these patterns with a significant block * hand * progress interaction ($X^2_8 = 88.3$; $p = 10^{-15}$). Post hoc tests indicated significant across-hand differences throughout the coarse delivery action in ΔGISI comparisons between B3 and B2 (onset, $\Delta\Delta GISI = -46.9 \pm 5.0$ mm; $z = -9.4$; $p < 0.0001$; AP_{25}, $\Delta\Delta GISI = -56.2 \pm 5.0$ mm; $z = -11.3$; $p < 0.0001$; AP_{50}, $\Delta\Delta GISI = -55.8 \pm 5.0$ mm; $z = -11.2$; $p < 0.0001$; AP_{75}, $\Delta\Delta GISI = -32.7 \pm 5.0$ mm; $z = -6.6$; $p < 0.0001$; offset, $\Delta\Delta GISI = -14.2 \pm 5.0$ mm; $z = -2.9$; $p = 0.01$) and between B3 and B1 (onset, $\Delta\Delta GISI = -22.8 \pm 5.0$ mm; $z = -4.6$; $p < 0.0001$; AP_{25}, $\Delta\Delta GISI = -42.2 \pm 5.0$ mm; $z = -8.5$; $p < 0.0001$; AP_{50}, $\Delta\Delta GISI = -60.4 \pm 5.0$ mm; $z = -12.1$; $p < 0.0001$; AP_{75}, $\Delta\Delta GISI = -45.1 \pm 5.0$ mm; $z = -9.1$; $p < 0.0001$; offset, $\Delta\Delta GISI = -25.4 \pm 5.0$ mm; $z = -5.1$; $p < 0.0001$). No significant hand differences were observed comparing B2 and B1 ($\Delta\Delta GISI = 2.0 \pm 2.2$ mm; $z = 0.9$; $p = 0.64$). These results are consistent with the coarse delivery results in Experiment 1.

Lastly, we evaluated eye–hand coordination during peg transport leading up to coarse delivery. A significant block * hand * progress interaction ($X^2_8 = 312.8$; $p = 10^{-16}$) captured the GISI dynamics which were characterized by smaller separations between gaze and the treated hand in the anesthesia block (Fig. 5*G*). Across-hand comparisons revealed significant differences in ΔGISI contrasting B3 and B2 at all AP points (onset, $\Delta\Delta GISI = -95.2 \pm 4.8$ mm; $z = -19.7$; $p < 0.0001$; AP_{25}, $\Delta\Delta GISI = -54.4 \pm 4.8$ mm; $z = -11.3$; $p < 0.0001$; AP_{50}, $\Delta\Delta GISI = -18.3 \pm 4.8$ mm; $z = -3.8$; $p = 0.0004$; AP_{75}, $\Delta\Delta GISI = -32.9 \pm 4.8$ mm; $z = -6.8$; $p < 0.0001$; offset, $\Delta\Delta GISI = -46.9 \pm 4.8$ mm; $z = -9.7$; $p < 0.0001$). Notably, the across-hand ΔGISI comparison comparing B2 to B1 failed achieved significance ($\Delta\Delta GISI = 0.4 \pm 2.2$ mm; $z = 0.2$; $p = 0.98$), indicating that sham injection did not affect the spatial relationship between the gaze and treated hand. More critically, the effect of anesthesia on gaze–hand relationships is consistent with the peg transport effects in Experiment 1.

Discussion

In this study, we examined eye–hand coordination during a dexterous motor task when fingertip somatosensation was acutely abolished. In two experiments, participants performed a unimanual pegboard task before and after digital anesthesia was administered to the thumb, index finger, and middle finger on one of the hands. We separated the task into placement and retrieval phases, each consisting of four specific actions: peg-free hand movement, peg collection, transport, and delivery. Because pegs were collected from and delivered to large and small holding containers, we examined whether somatosensory feedback loss impacted task performance in a manner that depended on specific actions according to their required precision. In both experiments, participants continued to complete the task successfully with insensate fingers, albeit with longer trial times and altered force profiles. When examining the gaze–hand spatial relationship throughout the task, we found that gaze was generally directed closer to the hand under anesthesia. Compensatory changes in gaze behavior reflected an adaptive strategy to maintain task performance by increasing visual monitoring

←

(sham). Blue data indicate GISI for the nondominant hand in Block 3. Red data indicate GISI for the dominant (anesthetized) hand in Block 3. ***D***, Lines and markers indicate mean GISI calculated as a function of progress (%) through the peg-free hand movement action. Conventions as in ***C***. ***E***, Bar plots showing the mean change in GISI at peak force during coarse delivery. Conventions as in ***B***. ***F***, Lines and markers indicate mean GISI calculated as a function of progress (%) through the coarse delivery action. Conventions as in ***C***. ***G***, Lines and markers indicate mean GISI calculated as a function of progress (%) through the peg transport action. Conventions as in ***C***. Force data for the retrieval phase of Experiment 2 is shown in Extended Data Figure 5-1. Summary statistics are provided in Extended Data Figure 5-2. Statistics of potential learning effects are provided in Extended Data Figure 5-3.

of the anesthetized hand. This compensation occurred when the dominant or nondominant hand was anesthetized and were significantly greater than the subtle changes observed in the sham injections. Because compensatory changes were evident in all task actions, even when no peg was grasped, we conclude that the acute removal of tactile feedback was associated with nonspecific modulation of eye–hand coordination.

We first determined whether digital anesthesia impacted performance on the pegboard task. Timing and force data revealed the importance of cutaneous responses to task performance (Extended Data Figs. 2-1, 2-2, 3-1, 3-2, 4-1, 4-2, 5-1, 5-2), consistent with earlier work (Augurelle et al., 2003; Monzée et al., 2003; Sober and Sabes, 2005; Trillos et al., 2018). First, participants took more time to complete collection and delivery following anesthesia, regardless of the precision required. The increased time required to complete the actions successfully could be due to altered manual dexterity resulting from the loss of cutaneous touch. Alternatively, but not exclusively, the increased time could reflect participants' switch to relying on visual feedback with the reasonable assumption that dexterous actions are slower when supported by visual feedback as compared with somatosensory feedback. Second, participants produced greater normal forces on the pegboard during all collection events and greater torque forces during precise collection events. Additionally, participants produced greater torque forces during precise delivery events. These results imply that somatosensory feedback is critical for force regulation. Lastly, peg transport times and peg-free hand movement were longer following anesthesia. These timing results suggest general adaptive changes that are not linked to specific task phases or even grasping, consistent with previous findings (Gentilucci et al., 1997). Collectively, these findings confirm that digital anesthesia impacted participants' ability to perform the pegboard task. Although participants were able to complete the task, the duration and force changes indicate that adaptations following the loss of somatosensory function only provided a partial rescue of function.

Our main finding was that digital anesthesia resulted in reduced spatial separation between gaze and hand position. This change in eye–hand coordination behavior was evident in all task actions. Following anesthesia, a smaller distance separated gaze and hand positions during collection and delivery actions, which suggests that participants relied more on visual feedback for peg interactions following the loss of somatosensory signals. The most obvious effect was seen with coarse collection where gaze is consistently close to the hand throughout the collection epoch in the anesthetized condition. In contrast, there was a greater gaze–hand separation in all other conditions that increases over the coarse collection epoch as participants looked away from the pegs and toward the upcoming placement targets. Gaze changes were more subtle with precise actions, which likely reflect a greater baseline demand for visual support of precise actions even with intact somatosensation. Indeed, gaze was closely tied to hand position during precise delivery and collection in all conditions, and anesthesia-related gaze changes were only evident at the end of the action. This pattern reflects vision's role in providing feedback regarding the success of peg collection or placement. However, with intact tactile sensation, vision was more quickly released from this feedback function, presumably to guide the upcoming hand movement (Blouin et al., 1996). This pattern is consistent with previous reports that different phases of prehension and movement can be performed without the necessity of visual feedback (Gentilucci et al., 1994). Notably, after digital anesthesia, we found that participants gazed longer at their hands through the actions rather than disengaging to support guidance for the upcoming movement. These collective results support a conceptual framework in which vision and somatosensation serve as action-phase controllers during dexterous manipulation tasks that require eye–hand coordination (Johansson et al., 2001) and imply that vision becomes essential for achieving task subgoals when tactile "checkpoints" are unreliable.

We found that participants continued to look closer to their hands during movement actions of the task following digital anesthesia. This effect was clearest with peg transport toward precise placement. Prior to anesthesia in the control conditions, gaze and hand behaviors appear to be independent. Accordingly, the transport action was characterized by a large initial separation between gaze and hand positions as participants looked toward the pegboard targets while independently completing peg collection. The gaze–hand separation gap then converged over the transport epoch as the peg was transported to the pegboard target where gaze was fixated. These results are consistent with previous studies suggesting that afferent information contributes to the adjustment between motor command and visual information (Vercher et al., 1996; Stenneken et al., 2006). We observed a different pattern with anesthesia: gaze remained closely tied to the hand throughout the transport action. This partially reflects the gaze–hand relationship during the preceding (collection) action, but it also reveals that participants looked closer to their hands as they transported the pegs, conceivably to monitor whether grasp was successfully maintained. We observed a similar pattern during transport toward coarse delivery, producing a behavior consistent with the hypothesis that vision is recruited to provide feedback when somatosensation is perturbed. Moreover, we found that during anesthesia, participants looked closer to their hands and needed more time in movement actions even when they were not grasping a peg. This surprising result implies that gaze behavior changes are not specifically tied to actions involving object interactions but also to the preparatory phase before object contact. Our study investigated the loss of sensory information on eye–hand coordination, and together our data support the notion that adaptation of eye–hand coordination following acute somatosensory feedback loss may be applied broadly rather than to specific actions.

We considered that the effects of digital anesthesia on task performance and compensatory behaviors may have depended on hand dominance. Conceivably, anesthesia effects could have been more pronounced with the nondominant hand assuming this hand is less dexterous. To address this possibility, we focused on the nondominant hand in Experiment 1 and the dominant hand in Experiment 2. In both experiments, performance with the dominant and

nondominant hands was comparable in the baseline blocks. More importantly, we found that anesthesia disrupted performance and induced gaze–hand changes in both experiments which indicates that the typical increased reliance on the dominant hand did not protect against the deleterious impacts of acute anesthesia.

In Experiment 2, we additionally tested the dominant hand after the participants received a sham injection. This manipulation allowed us to determine whether the mere experience of receiving an injection – with sensation left intact or even heightened – could have altered the salience of the hand and participants' use of the hand. Across task phases, gaze behavior following sham injection mostly matched baseline behavior, although there were subtle differences in some actions. Notably, the gaze–hand separation in some actions "increased" following sham injection compared with the baseline, suggesting that participants relied "less" on their gaze as they gained experience on the task. Indeed, we found a significant block * hand interaction in the collect and delivery actions in the placement phase and the collection action in the retrieval phase, which is consistent with learning effects within the blocks (Wolpert and Flanagan, 2010). Motivated by these observations, we performed exploratory analyses to quantify potential learning effects. We tested whether the duration of force application and GISI at peak force changed within each block for each hand separately (Extended Data Figs. 2-3, 3-3, 4-3, 5-3). Although we found significant linear trends in some conditions, these effects were inconsistent across experiments and tended to be small. Some trends followed learning effect predictions (i.e., shorter force durations and increased GISI over series); however, trends in the opposite direction were also observed. Crucially, any changes in force duration or GISI associated with potential learning effects were substantially smaller than digital anesthesia effects. The effects of sham and anesthesia matched in direction (i.e., reduced gaze–hand separation) only during the peg-free movements of the retrieval phase (Fig. 5*D*, right), but the significant sham effects may have been related to the disproportionately large gaze–hand separations with the dominant hand in the baseline block. In all analyses, the influence of anesthesia on gaze–hand relationships dwarfed those seen with sham injection or learning.

While the effects shown in this study are clear, further experimental modifications can improve the paradigm and expand the findings. First, we have a limited sample size with gaze data from 10 participants across two experimental groups. However, by testing each participant extensively, with 1,280 trials per participant in Experiment 1 and 1,920 trials per participant in Experiment 2, we systematically determined each participant's performance with and without digital anesthesia with robustness. Our data revealed robust effects of anesthesia that replicated over two independent experiments. Although there were subtle individual differences that likely reflected the strategies employed to complete the task, we leveraged this variance in our models which included trial-level data from the experimental and control hands of each subject. Despite confidence in the results of our small-sampled experiments, the generalizability of our conclusions must be evaluated in future studies with larger samples. Next, in applying digital anesthesia to the fingers, the positional sense of fingers may have been affected in addition to the cutaneous sensibilities. Because of the importance of proprioception to prehension and grasping (Gentilucci et al., 1997), the sensitivity of cutaneous mechanoreceptors to hand kinematics (Edin and Abbs, 1991), and modulatory influence of cutaneous vibrations on proprioceptive acuity (Weerakkody et al., 2007), perturbed proprioception may have contributed to the disrupted performance on our task. We neglected to evaluate position sense with the anesthetized fingers, so the role of proprioception (loss) in gaze–hand adaptation remains to be tested. Furthermore, we did not track the nonanesthetized fingers, and participants may have shifted their gaze to these fingers. We think this is unlikely for multiple reasons. First, due to the natural hand orientation during the task, these fingers were partially occluded by the radial digits. Second, continuous visual monitoring by the experimenter also confirmed that these fingers did not participant in grasping the pegs in any of the trials. However, without direct quantification of finger-specific gaze allocation or visibility, we cannot rule out the influence of neighboring finger movement. Third, the lack of consistent trial structure, particularly with respect to the peg order that participants needed to complete the delivery and collection actions, precluded us from careful analysis into the pattern of gaze behavior based on pegboard position. Future studies incorporating a systematic peg selection order may better assess the impact of visuomotor strategy on eye–hand coordination behavior and motor planning. Lastly, our analyses of gaze–hand relationships were handicapped by the limited sampling rate of our gaze tracking system. With a higher sampling rate, more sensitive dynamics in gaze–hand coordination may be observed.

In conclusion, we found that the loss of somatosensory feedback through digital anesthesia impairs performance on a manual dexterity task. Learning effects from previous experience with the task were lost following anesthesia, and behavioral adaptations only partially rescued performance. To compensate for the loss of touch, participants consistently directed their gaze closer to their hands, which we interpret as the recruitment of vision for feedback functions typically supported by touch. That gaze became more closely tied to the hands following anesthesia even in the absence of peg grasping implies that adaptations to dexterous behaviors may be more general in nature. Although our results reveal that gaze–hand behavior adaptations generalize across task phases in our paradigm, an open question is whether they would extend to other tasks. Future studies can address this question as well as whether our compound eye–hand coordination assessment technique can reveal adaptations in persons that suffer from chronic somatosensory feedback impairment. Similarly, this approach provides biomarkers of adaptive changes after peripheral nerve injury affecting sensation in the hand and offers a valuable tool for assessing the impact of clinical interventions aimed at restoring function. Clinicians can track these mechanisms to evaluate recovery after nerve repair and compare treatments. Such insights are crucial for translating sensorimotor research into clinical applications, ultimately enhancing outcomes for individuals with

sensory deficits or motor impairments. Future work could determine whether the effect of learning persists after tactile feedback has returned, shedding light on the durability of sensorimotor adaptations. Finally, expanding our understanding of how dexterous behavior patterns change with altered somatosensory and visual feedback may also inform the design of neuroprosthetics and optimize training regimens for advanced robotic telesurgery.

References

Augurelle A-S, Smith AM, Lejeune T, Thonnard J-L (2003) Importance of cutaneous feedback in maintaining a secure grip during manipulation of hand-held objects. J Neurophysiol 89:665–671.

Bates D, Mächler M, Bolker B, Walker S (2015) Fitting linear mixed-effects models using lme4. J Stat Softw 67:1–48.

Bilaloglu S, Lu Y, Geller D, Ross Rizzo J, Aluru V, Gardner EP, Raghavan P (2016) Effect of blocking tactile information from the fingertips on adaptation and execution of grip forces to friction at the grasping surface. J Neurophysiol 115:1122–1131.

Birznieks I, Burstedt MKO, Edin BB, Johansson RS (1998) Mechanisms for force adjustments to unpredictable frictional changes at individual digits during two-fingered manipulation. J Neurophysiol 80:1989–2002.

Blouin J, Gauthier GM, Vercher J-L, Cole J (1996) The relative contribution of retinal and extraretinal signals in determining the accuracy of reaching movements in normal subjects and a deafferented patient. Exp Brain Res 109:148–153.

Caplan B, Mendoza JE (2011) Edinburgh handedness inventory. In: Encyclopedia of clinical neuropsychology (Kreutzer JS, DeLuca J, Caplan B, eds), pp 928. New York: Springer.

Chesler AT, et al. (2016) The role of *PIEZO2* in human mechanosensation. N Engl J Med 375:1355–1364.

Cuadra C, Falaki A, Sainburg R, Sarlegna FR, Latash ML (2019) Case studies in neuroscience: the central and somatosensory contributions to finger interdependence and coordination: lessons from a study of a "deafferented person". J Neurophysiol 121:2083–2087.

Edin BB, Abbs JH (1991) Finger movement responses of cutaneous mechanoreceptors in the dorsal skin of the human hand. J Neurophysiol 65:657–670.

Fox J, Weisberg S, Price B (2001) Car: companion to applied regression. In: *CRAN: contributed packages*.

Gentilucci M, Toni I, Chieffi S, Pavesi G (1994) The role of proprioception in the control of prehension movements: a kinematic study in a peripherally deafferented patient and in normal subjects. Exp Brain Res 99:483–500.

Gentilucci M, Toni I, Daprati E, Gangitano M (1997) Tactile input of the hand and the control of reaching to grasp movements. Exp Brain Res 114:130–137.

Gordon AM, Westling G, Cole KJ, Johansson RS (1993) Memory representations underlying motor commands used during manipulation of common and novel objects. J Neurophysiol 69:1789–1796.

Jenmalm P, Johansson RS (1997) Visual and somatosensory information about object shape control manipulative fingertip forces. J Neurosci 17:4486–4499.

Jenmalm P, Dahlstedt S, Johansson RS (2000) Visual and tactile information about object-curvature control fingertip forces and grasp kinematics in human dexterous manipulation. J Neurophysiol 84:2984–2997.

Jenmalm P, Birznieks I, Goodwin AW, Johansson RS (2003) Influence of object shape on responses of human tactile afferents under conditions characteristic of manipulation. Eur J Neurosci 18:164–176.

Johansson RS, Flanagan JR (2009) Coding and use of tactile signals from the fingertips in object manipulation tasks. Nat Rev Neurosci 10:345–359.

Johansson RS, Westling G (1984) Roles of glabrous skin receptors and sensorimotor memory in automatic control of precision grip when lifting rougher or more slippery objects. Exp Brain Res 56:550–564.

Johansson RS, Westling G (1987) Signals in tactile afferents from the fingers eliciting adaptive motor responses during precision grip. Exp Brain Res 66:141–154.

Johnson KO, Hsiao SS (1992) Neural mechanisms of tactual form and texture perception. Annu Rev Neurosci 15:227–250.

Johansson RS, Westling G, Bäckström A, Flanagan JR (2001) Eye–hand coordination in object manipulation. J Neurosci 21:6917–6932.

Killick R, Fearnhead P, Eckley IA (2012) Optimal detection of changepoints with a linear computational cost. J Am Stat Assoc 107:1590–1598.

Lenth RV (2017) Emmeans: estimated marginal means, aka least-squares means. In: *CRAN: contributed packages*.

Lukos J, Ansuini C, Santello M (2007) Choice of contact points during multidigit grasping: effect of predictability of object center of mass location. J Neurosci 27:3894–3903.

Mahmud AA, et al. (2017) Loss of the proprioception and touch sensation channel PIEZO2 in siblings with a progressive form of contractures. Clin Genet 91:470–475.

Monzée J, Lamarre Y, Smith AM (2003) The effects of digital anesthesia on force control using a precision grip. J Neurophysiol 89:672–683.

Nordmark PF, Ljungberg C, Johansson RS (2018) Structural changes in hand related cortical areas after median nerve injury and repair. Sci Rep 8:4485.

Rao A, Gordon A (2001) Contribution of tactile information to accuracy in pointing movements. Exp Brain Res 138:438–445.

Sailer U, Flanagan JR, Johansson RS (2005) Eye–hand coordination during learning of a novel visuomotor task. J Neurosci 25:8833–8842.

Sathian K, Goodwin A, John K, Darian-Smith I (1989) Perceived roughness of a grating: correlation with responses of mechanoreceptive afferents innervating the monkey's fingerpad. J Neurosci 9:1273–1279.

Searle SR, Speed FM, Milliken GA (1980) Population marginal means in the linear model: an alternative to least squares means. Am Stat 34:216–221.

Sober SJ, Sabes PN (2005) Flexible strategies for sensory integration during motor planning. Nat Neurosci 8:490–497.

Stenneken P, Prinz W, Cole J, Paillard J, Aschersleben G (2006) The effect of sensory feedback on the timing of movements: evidence from deafferented patients. Brain Res 1084:123–131.

Trillos M-C, Soto F, Briceno-Ayala L (2018) Upper limb neurodynamic test 1 in patients with clinical diagnosis of carpal tunnel syndrome: a diagnostic accuracy study. J Hand Ther 31:333–338.

Vercher JL, Gauthier GM, Guedon O, Blouin J, Cole J, Lamarre Y (1996) Self-moved target eye tracking in control and deafferented subjects: roles of arm motor command and proprioception in arm-eye coordination. J Neurophysiol 76:1133–1144.

Weerakkody NS, Mahns DA, Taylor JL, Gandevia SC (2007) Impairment of human proprioception by high-frequency cutaneous vibration. J Physiol 581:971–980.

Winges SA, Weber DJ, Santello M (2003) The role of vision on hand preshaping during reach to grasp. Exp Brain Res 152:489–498.

Wolpert DM, Flanagan JR (2010) Motor learning. Curr Biol 20:R467–R472.

Yahya A, Kluding P, Pasnoor M, Wick J, Liu W, dos Santos M (2019) The impact of diabetic peripheral neuropathy on pinch proprioception. Exp Brain Res 237:3165–3174.